Evaluation of Sea Surface Winds and Waves Retrieved From the Chinese HY-2B Data

Weizeng Shao, *Member, IEEE*, Tao Jiang, Xingwei Jiang, Youguang Zhang, and Wei Zhou

***Abstract*—The wind and wave derived from the scatterometer and altimeter on board the Chinese Haiyang-2B (HY-2B) satellite were systemically evaluated in this article. The analysis of matchups between advanced scatterometer and the winds from HY-2B scatterometer with wind speeds up to 25 m/s showed a 0.78 m/s root-mean-square error (RMSE) with a 0.97 correlation (COR), superior to the 1.2 m/s RMSE and 0.93 COR of winds from the altimeter of HY-2B. Simultaneously, significant wave heights (SWHs) measured from HY-2B were collocated with measurements from the Jason-3 altimeter. Analysis of the calibration concluded that the observations from the HY-2B altimeter performed well at low-to-moderate sea states, yielding an RMSE of 0.29 m for SWH with a 0.98 COR for geophysical data records (GDRs) data after systematic corrections using the MOE determination method. In particular there were 20 typhoons occurring in China Seas during 2019–2020. The evaluation of high SWH when compared with those (SWH $>$ 7 m) from Jason-3/WW3 indicated that HY-2B is accurate, with a 0.87 m/0.68 m RMSE and a 0.85 COR with SWH. Finally, statistical analysis of wind speed and SWH was investigated through waves simulated from the WAVEWATCH-III (WW3)/hybrid coordinate ocean using the current and the sea surface temperature (SST). The HY-2B wind measurements performed well at sea surface currents below 1 m/s and SWH less than 3 m, while a term for SST should be included in the scatterometer wind speed retrieval. In addition, wave states likely affect the accuracy of HY-2B wave speed measurements.**

***Index Terms*—Haiyang-2B (HY-2B), sea surface waves, sea surface winds, typhoon condition.**

I. Introduction

THE chinese marine monitoring satellite Haiyang-2B (HY-2B) was successfully launched in October 2018, and operational sea surface wind and wave measurement data products were officially released by the National Satellite Ocean Application Service (NSOAS). At present several types of remote-sensing data products are available for global oceanography research; e.g., winds from the advanced scatterometer (ASCAT) on board METOP [1] and the WindSat Polarimetric Radiometer [2], and waves from the Jason-2 altimeter [3] and synthetic aperture radar (SAR) [4]. These data have been calibrated against moored buoys at various sea states [5]–[7]. The HY-2A satellite was launched in 2011 and is capable of monitoring marine dynamics, i.e., sea surface winds, waves, currents, tides, and sea surface temperature (SST). Haiyang-1 (HY-1) is the first Chinese satellite operating at an optical frequency for oceanography research, and the applicability of HY-1A has been well studied [8]–[10] during the past ten years. Typically, HY-2B carries three sensors at microwave frequency; i.e., a scatterometer having four radar beams at incidence angles of 41.4° and 48.5°, a radar altimeter [11], and a microwave radiometer, which can provide both wind and wave data. The sun-synchronous orbital period of HY-2B is approximately 104 minutes at about 970 kilometers of flight height; therefore, it can cover 90% of the global ocean in a day. Efforts have been made to derive reliable sea surface wind fields from the scatterometer using a well-known model of the geophysical function (GMF) [12], [13]. This model describes an empirical relation between a wind vector and radar backscattering signals represented by a radar cross section (RCS) based on Bragg wave backscattering theory. Because HY-2B operates at a Ku-band ($\sim$13.2 GHz), similar to the *C*-band GMF [14], a Ku-band GMF NSCAT-4 [15] was developed for inverting the sea surface wind data from the scatterometer in vertical-vertical and horizontal-horizontal polarizations. Unfortunately, two unknown variables, wind speed and direction, are unable to be resolved by one function. Under these circumstances the RCSs are measured at two incidence angles, 41° and 48°. It has been demonstrated that the accuracy of scatterometer-measured wind speed is about 2 m/s for QuikSCAT [16] and ASCAT [17].

The three-month mission of SEASAT in 1979 yielded insights concerning satellite wave observations [18]. The ocean surface waves are measured by the altimeter of HY-2B. The incidence angle of the altimeter is within 2°; therefore, the backscattering signal associated with the mean-square sea surface slope is determined by specular reflection [19]. The sea state measured from the altimeter is the total sea surface height (SSH) [20] combined with the sea surface wave, tide, and sea level. The algorithms that retrieve the significant wave height (SWH) [21] are a mature technology based on the retraced backscattering waveform, e.g.,

Manuscript received April 29, 2021; revised September 3, 2021; accepted September 12, 2021. Date of publication September 16, 2021; date of current version October 6, 2021. This work was supported in part by the National Key Research and Development Program of China under Grant 2017YFC1404000, in part by the Key Special Project for Introduced Talents Team of Southern Marine Science and Engineering Guangdong Laboratory (Guangzhou) under Grant GML2019ZD0302, in part by the National Natural Science Foundation of China under Grant 42076238, and in part by China Postdoctoral Science Foundation under Grant 2020M670245. *(Corresponding author: Weizeng Shao.)*

Weizeng Shao is with the College of Marine Sciences, Shanghai Ocean University, Shanghai 201306, China, and also with National Satellite Ocean Application Service, Shanghai 201306, China (e-mail: shaoweizeng@mail.tsinghua.edu.cn).

Tao Jiang is with Shanghai Ocean University, Shanghai 201306, China (e-mail: m200200560@st.shou.edu.cn).

Xingwei Jiang is with Southern Marine Science and Engineering Guangdong Laboratory (Guangzhou), Guangzhou 511458, China (e-mail: xwjiang@mail.nsoas.org.cn).

Youguang Zhang is with National Satellite Ocean Application Service, Beijing 100081, China (e-mail: zhangyouguang@mail.nsoas.org.cn).

Wei Zhou is with the South China Sea Institute of Oceanology, Chinese Academy of Sciences, Guangzhou 510301, China (e-mail: zhouwei@scsio.ac.cn).

Digital Object Identifier 10.1109/JSTARS.2021.3112760

the physics-based model Beta5 [22] and empirical model OCOG [23]. It is revealed that the accuracies of SSH and SWH are approximately 0.05 m [24] and 0.4 m [25], respectively. For wave retrieval from the HY-2B altimeter, the four-parameter tracking method is used to retrace the waveform, and then the Brown model [26], [27] is employed to retrieve SWH, similar to the procedure for the Jason altimeter. Moreover, sea surface winds are also obtained from the HY-2B altimeter using an empirical model of altimeter wind speed that considers the effect of the sea state [28].

In this article, the HY-measured wind and wave data were collected during the period from January 2019 to October 2020. The HY-2B altimeter provides four types of data products at Level-2 (L2); i.e., operational geophysical data records (OGDR), interim geophysical data records (IGDR), sensor geophysical data records (SGDRs), and geophysical data records (GDR). Two well-calibrated measurements, ASCAT winds and Jason-2 waves, were collected in order to calibrate the operational data from the HY-2B scatterometer and altimeter, respectively. The global and regional assimilation and prediction system (GRAPS) [29] and the WAVEWATCH-III (WW3) [30]–[32] model were also collocated with HY-2B data. In particular those model-simulated results are available for investigating the performance of HY-2B in monitoring typhoons.

The rest of this article is organized as follows. Section II briefly describes the datasets available for this article, i.e., HY-2B data, ASCAT winds, Jason-3 waves, and hybrid coordinate ocean model (HYCOM) current field and SST data [33]. Using simulations derived from GRAPS and WW3 models is also confirmed. Section IV presents the calibration results of HY-2B winds and waves in low-to-moderate sea states over the global ocean and typhoons in the China Seas. The statistical analyses of HY-measured wind speed and SWH are discussed in Section IV. Finally, Section V concludes this article.

II. Description of the Dataset

The HY-2B satellite carries two microwave sensors: a scatterometer and an altimeter. The wind measurements are operationally provided by NSOAS up to 25 km spatial resolution twice per day. As an example, Fig. 1 shows the wind vector maps for July 16, 2020 in the western Pacific Ocean, in which there are a few gaps in the swath coverage. Similarly, four types of wind and wave product measurements derived from the HY-2B altimeter, i.e., OGDR, IGDR, SGDR, and GDR, can also be accessed through an authorized account for worldwide investigators. Specifically, OGDR and IGDR measurements are the real-time measurements without systematic corrections by using real-time accuracy orbit ephemeris and medium accuracy orbit ephemeris (MOE) determination methods. SGDR and GDR measurements are the data after systematic corrections by using MOE and precise orbit ephemeris determination. Note that HY-2B OGDR data were only available for June to October 2020. The HY-measured SWH map of GDR measurements with overlaid water depth in July 2020 is presented in Fig. 2.

In order to calibrate the HY-2B winds ASCAT winds on board the new-generation all-weather European active microwave scatterometer METOP were employed; these are normally used for

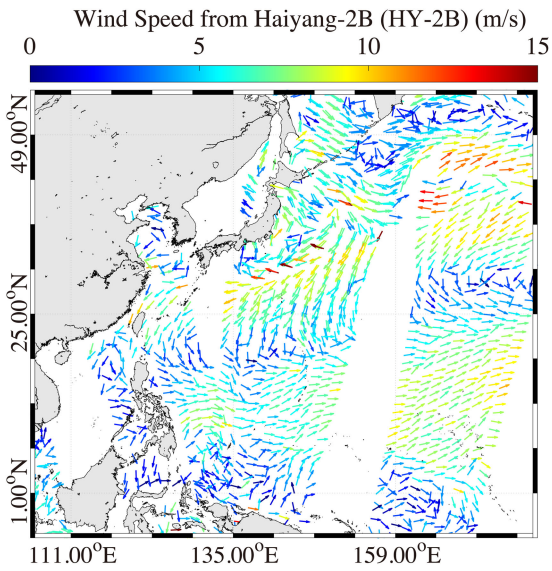

Fig. 1. Wind vector map derived from the scatterometer of HY-2B on July 16, 2020.

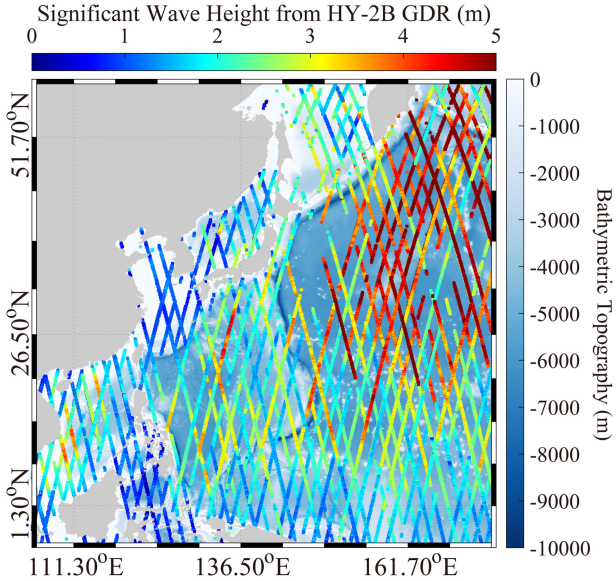

Fig. 2. SWH map derived from the altimeter of HY-2B geophysical data records overlaid with the water depth for July 2020.

the calibration of other remote-sensing retrievals (e.g., SAR [34], [35]). ASCAT wind with an 1800-km-wide swath was operationally released in February 2007, and its performance has been investigated, showing that the error is below 1 m/s [36]. In this article, the spatial resolution of ASCAT winds was about 25 km, and the time difference between the ASCAT and HY-2B values was within two hours. Note that the backscattering returns from the scatterometer suffer from the saturation problem [37] at strong winds ($>\sim$25 m/s) as well as SAR [38]; thus, we used for our research the ASCAT winds less than 25 m/s. The satellite Jason-3 launched by the National Oceanic and Atmospheric Administration in January 2016 is the successor to the Jason-2 mission. Jason-3 is an international cooperation with the Centre National d'Etudes Spatiales, European Organisation for

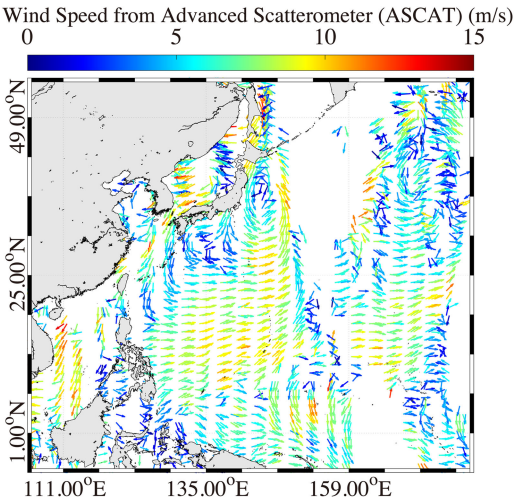

Fig. 3. Wind vector map derived from the ASCAT during July 15–18, 2020.

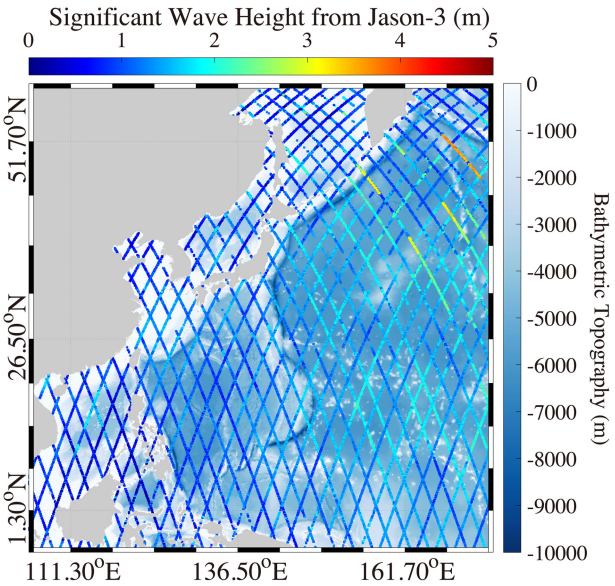

Fig. 4. SWH map derived from the altimeter of Jason-3 overlaid with the water depth in July 2020.

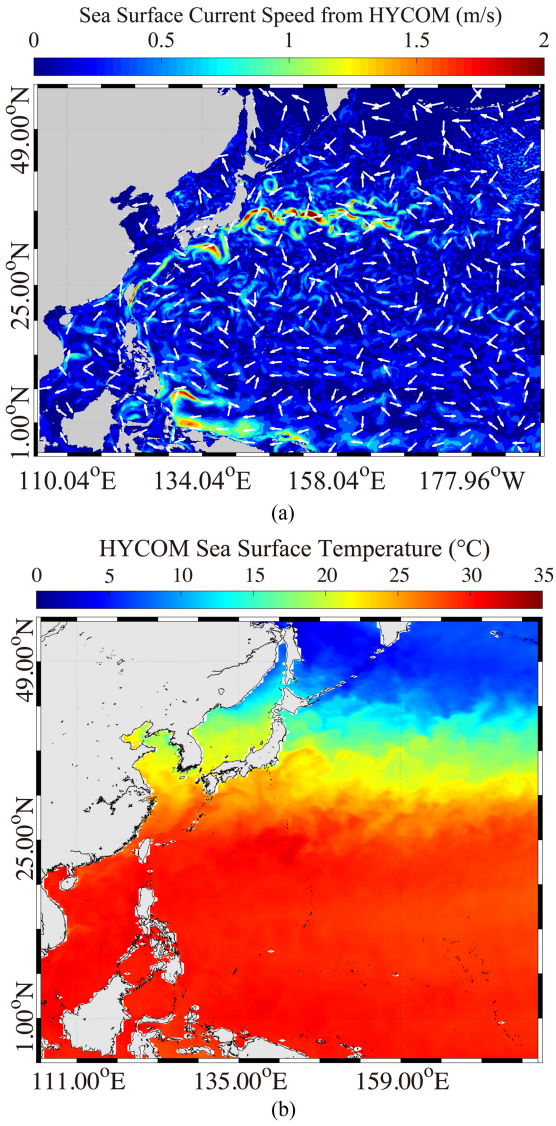

Fig. 5. (a) HYCOM sea surface current map at 12:00 UTC on 17 June 2020. (b) HYCOM SST map at 12:00 UTC on 17 June 2020.

the Exploitation of Meteorological Satellites, and the National Aeronautics and Space Administration (NASA). Global SWH measurements from the Jason-3 mission were matched with those from the HY-2B altimeter in maintaining the SWH, which was measured by following the footprints (∼10 km) of the satellite. The time difference between the Jason-3 and HY-2B values was within 1.5 h, and the distance difference was less than 3 km. As examples, Fig. 3 shows the wind vector map derived from ASCAT during July 15–18, 2020, and Fig. 4 shows the SWH map derived from the altimeter of Jason-3 overlaid with the water depth in July 2020.

The wave fields in the western Pacific ocean were also simulated by the WW3 model; in particular, winds from GRAPS were treated as the forcing fields, which are officially released by the China Meteorological Administration of the National Climate Center. The spatial resolution of GRAPS wind speed is about 3 km at intervals of 1 h. As pointed out in [31] and [39], sea surface currents play important roles in the wave simulation at coastal waters, especially for typhoons. Therefore, the HYCOM sea surface current at a 0.08° grid at intervals of 3 h were the open boundary conditions. In addition, the SST was used for analyzing the statistical errors of the measurements of HY-2B. The HYCOM current and SST maps at 12:00 UTC on 17 June 2020 are shown in Fig. 5. The specific settings of the WW3 model in this article are as follows.

1) The general bathymetric chart of the oceans water depth with a spatial resolution of ∼1 km in the horizontal direction.
2) The frequency bins ranged from 0.04118 to 0.7186 at an interval of $\Delta f/f = 0.1$.
3) The time step was set by default to be 300 s in both the longitudinal and latitudinal directions.
4) The two-dimensional wave spectrum is resolved into 24 regular azimuthal directions at intervals of 15°.

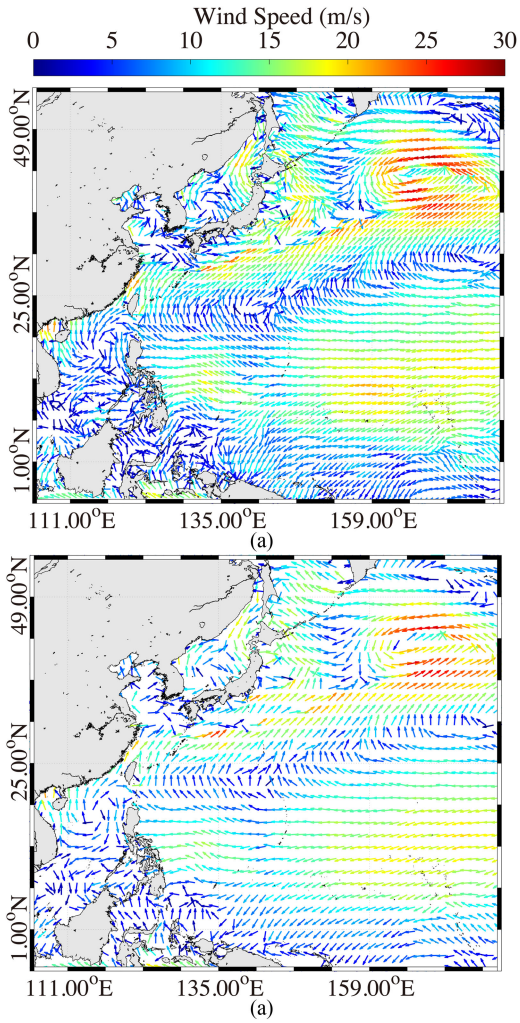

Fig. 6. (a) GRAPS wind map at 12:00 UTC on June 16, 2020. (b) ECMWF wind map at 12:00 UTC on June 16, 2020.

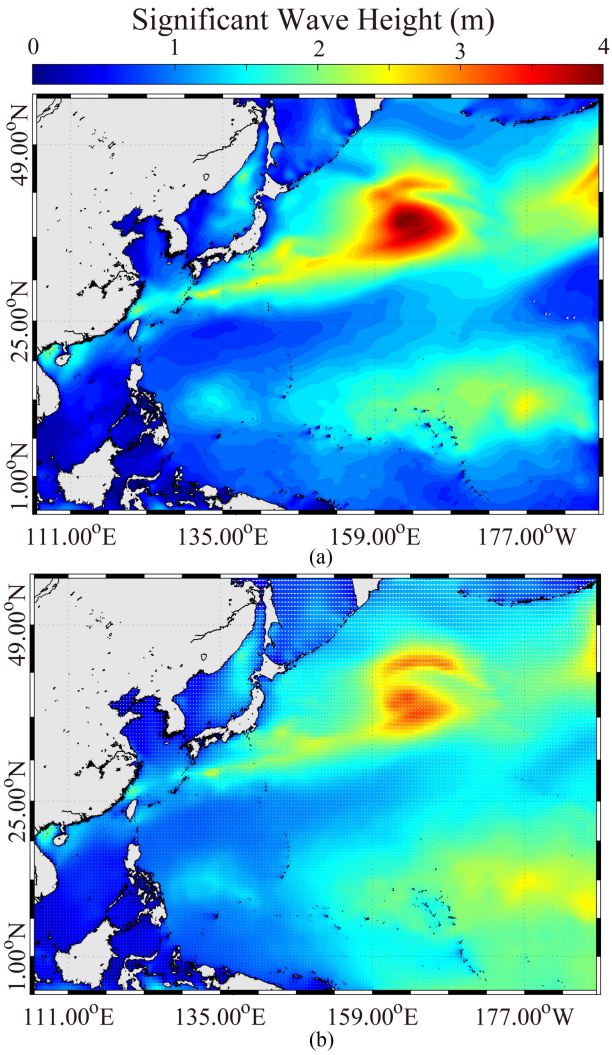

Fig. 7. (a) WW3-simulated SWH map at 12:00 UTC on June 16, 2020. (b) ECMWF SWH map at 12:00 UTC on June 16, 2020.

5) The parameters of the energy input and dissipation terms, referred to as ST2 and STAB2 in [30], were selected.
6) The nonlinear term for the quadratic wave–wave interactions package, named the generalized multiple discrete interaction approximation, was selected [40].
7) SWH outputs were at a 0.1° grid with a 30-min temporal resolution.

Since 1979 the European Centre for Medium-Range Weather Forecasts (ECMWF) has continuously provided various datasets, including atmospheric and oceanic parameters assimilated with buoy observations and remote-sensed measurements for scientific research. The spatial resolution of ECWMF reanalysis data uses 0.5° grids at an interval of 1 h, which is relatively coarser than GRAPS wind and WW3-simulated SWH. ECMWF data were employed to confirm the applicability of model-simulated winds and waves. Fig. 6(a) and (b) shows GRAPS and ECMWF wind maps at 12:00 UTC on 16 June 2020. Similarly, Fig. 7(a) and (b) shows WW3 and ECMWF SWH maps at 12:00 UTC on 16 June 2020. It is clear from the figures that the patterns between ECMWF data and WW3-simulated SWHs are consistent; in particular, the model simulations show more detail. The comparisons between ECMWF and model simulations showed a 0.96 m/s root-mean-square error (RMSE) of wind speed with a 0.92 correlation (COR) [see Fig. 8(a)] and a 0.47 m RMSE of SWH with a 0.81 COR [see Fig. 8(b)]. By analyzing ECMWF wind over the global ocean, we find that the ECMWF tended to underestimate speeds [41]; this was improved to some extent for WW3-simulated SWHs by using GRAPS winds. Under these circumstances we believe that the sea states from the WW3 model in 2019–2020, even during typhoons, are reliable for this article. The tracks of typhoons available for this article are presented in Fig. 9.

III. Results

A. Validation at Low-to-Moderate Sea Sates

The SWH and sea surface wind field of HY-2B satellite have been calibrated using field measurements from Wanshan altimeter calibration field and National Data Buoy Center buoys. The measurements from the HY-2B scatterometer during the two-year mission were collocated with those from ASCAT and

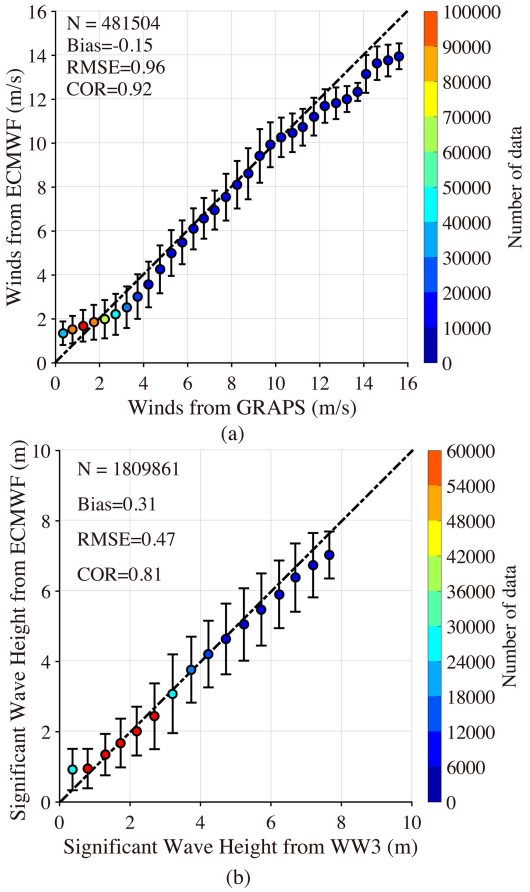

Fig. 8. (a) Comparisons between GRAPS and ECMWF wind speeds for a 0.5 m/s bin. (b) Comparisons between WW3 and ECMWF SWHs for a 0.5 m bin.

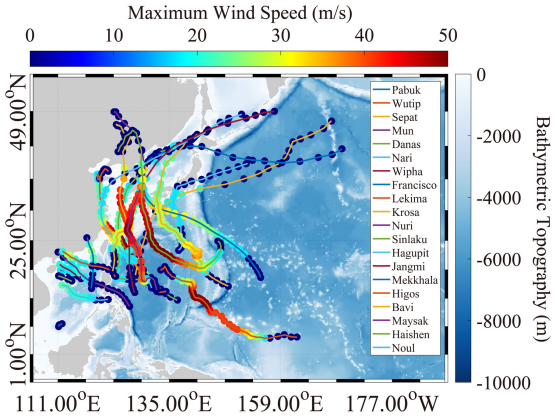

Fig. 9. Tracks of typhoons passing the China Seas in 2019–2020 overlaid with the water depth.

Jason-3, where the time difference was within 1.5 h and the spatial coverage difference was within 3 km. We have more than one hundred thousand matchups with wind speed up to 25 m/s, showing a 0.78 RMSE with a 0.97 COR, as shown in Fig. 10. Similarly, the winds from the altimeter of HY-2B were also calibrated against ASCAT winds, although only about 60 points were available due to the coarse spatial resolution of the HY-2B altimeter (∼10 km in the horizontal direction). Fig. 11

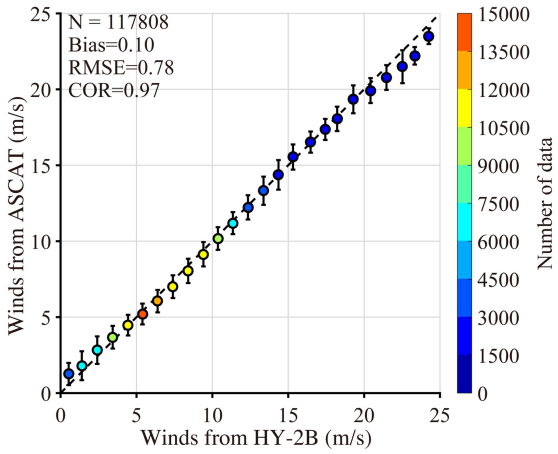

Fig. 10. Comparisons of wind speeds between HY-2B and ASCAT for a 0.5 m/s bin.

presents the comparisons for four data product types from the HY-2B altimeter, yielding approximately 1.2 m/s RMSE with a 0.94 COR. Moreover, winds from the HY-2B altimeter generally tended to overestimate speeds compared to ASCAT winds. The comparisons of wind speeds between GRAPS and HY-2B are shown in Fig. 12, indicating similar analysis results.

The SWHs from four types of measurements from the HY-2B altimeter were compared with measurements from Jason-3 at low-to-moderate sea states (SWH $<$ 7 m) over the global ocean (see Fig. 13), where SWH ranged from 0 to 7 m for a 0.5 m bin. Generally, although SWH data were reliable, yielding an approximate 0.3 m RMSE and 0.98 COR, the GDR data performed better, with a 0.29 m RMSE and 0.98 COR with SWH. This behavior was also observed by comparison of SWHs with the simulations from the WW3 model in the western Pacific ocean (see Fig. 14). However, the error was relatively large (about 0.5 m RMSE and 0.92 COR) at high sea states (5 m $<$ SWH $<$ 11 m). Therefore, the accuracy of HY-measured SWH was studied at higher sea states such as during typhoons.

B. *Validation in Typhoons*

During the past two years 20 typhoons passing through the China Seas were captured by HY-2B. Because the scatterometer suffers saturation problems at strong wind speeds (>25 m/s), the performance of the HY-2B altimeter at high sea states (7 m $<$ SWH $<$ 14 m) was investigated for those typhoons. The matchups from HY-2B were calibrated against the collocated SWHs from Jason-3 for more than 200 samples, as illustrated in Fig. 14. There are fewer data values (<100 samples) for HY-2B OGDR during the period from June to October 2020; these are not presented here. Generally, HY-measured SWHs were lower than observations from Jason-3, and the bias (HY-2B minus Jason-3) was equal to −0.51 m for IGDR and SGDR measurements. In addition, the RMSE of SWH was about 0.95 m for IGDR and SGDR products, whereas a 0.87 m RMSE was achieved for GDR data, and the bias was reduced to −0.32 m. However, the error became scattered at SWH greater than 10 m due to insufficient samples. The measurements were also

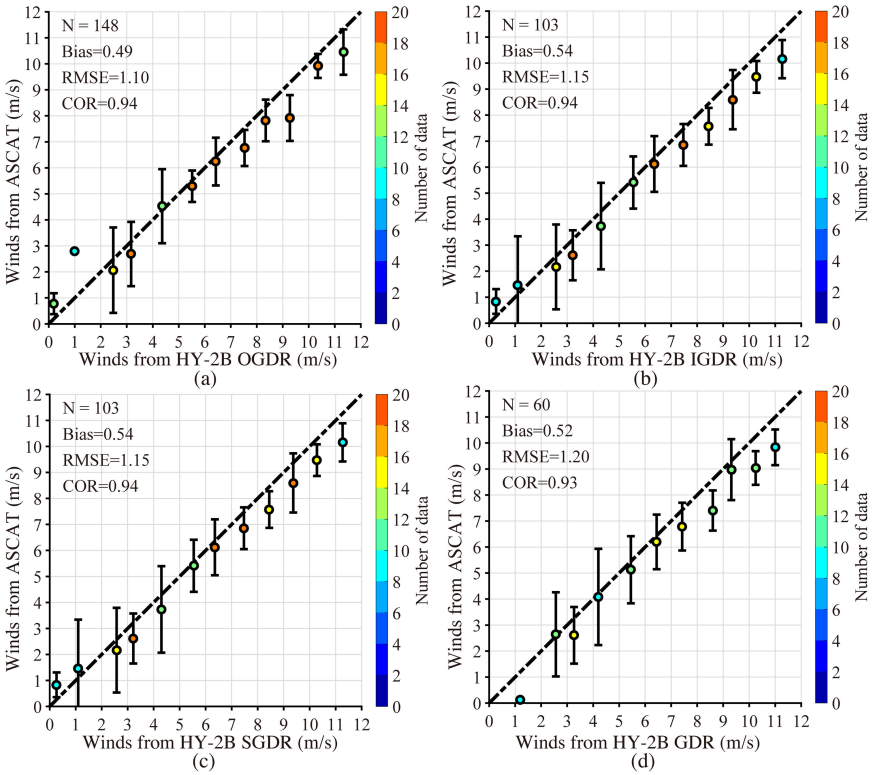

Fig. 11. Comparisons of wind speeds between ASCAT and HY-2B for a 0.5 m/s bin. (a) Operational geophysical data records. (b) Interim geophysical data records. (c) Sensor geophysical data records. (d) Geophysical data records.

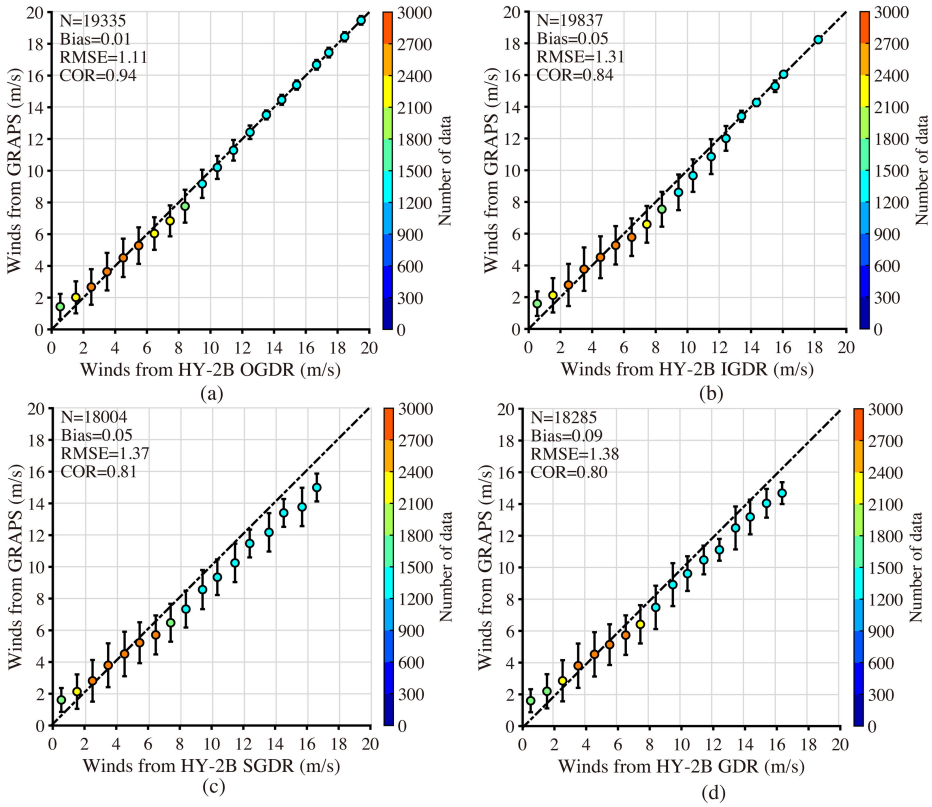

Fig. 12. Comparisons of wind speeds between GRAPS and HY-2B for a 0.5 m/s bin. (a) Operational geophysical data record. (b) Interim geophysical data record. (c) Sensor geophysical data record. (d) Geophysical data record.

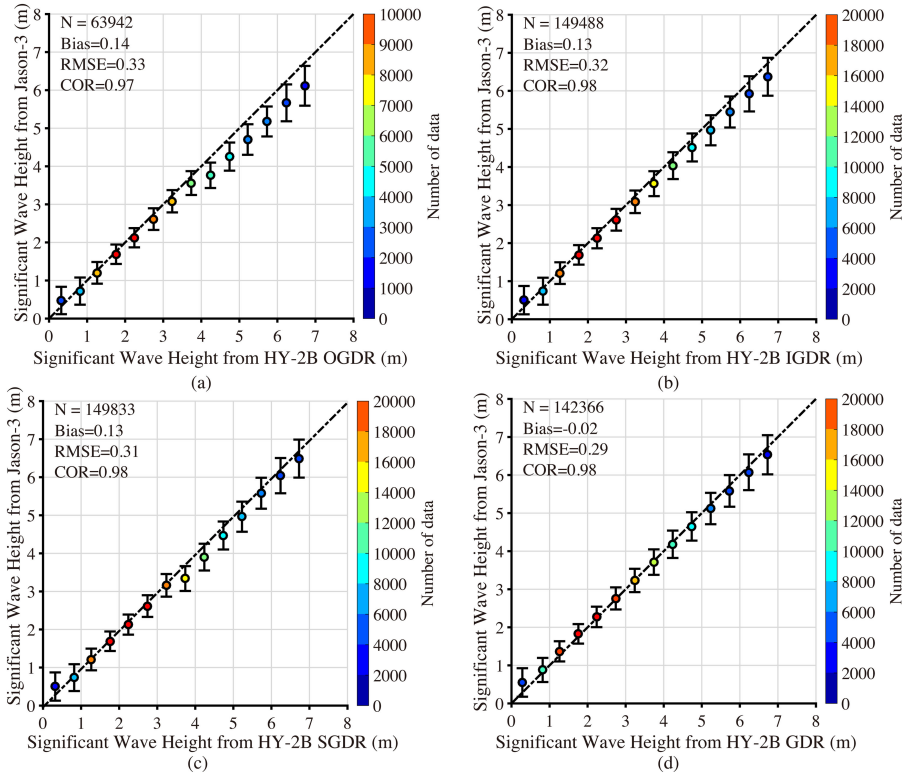

Fig. 13. Comparisons of SSH between Jason-3 and HY-2B for a 0.5 m bin. (a) Operational geophysical data record. (b) Interim geophysical data record. (c) Sensor geophysical data record. (d) Geophysical data record.

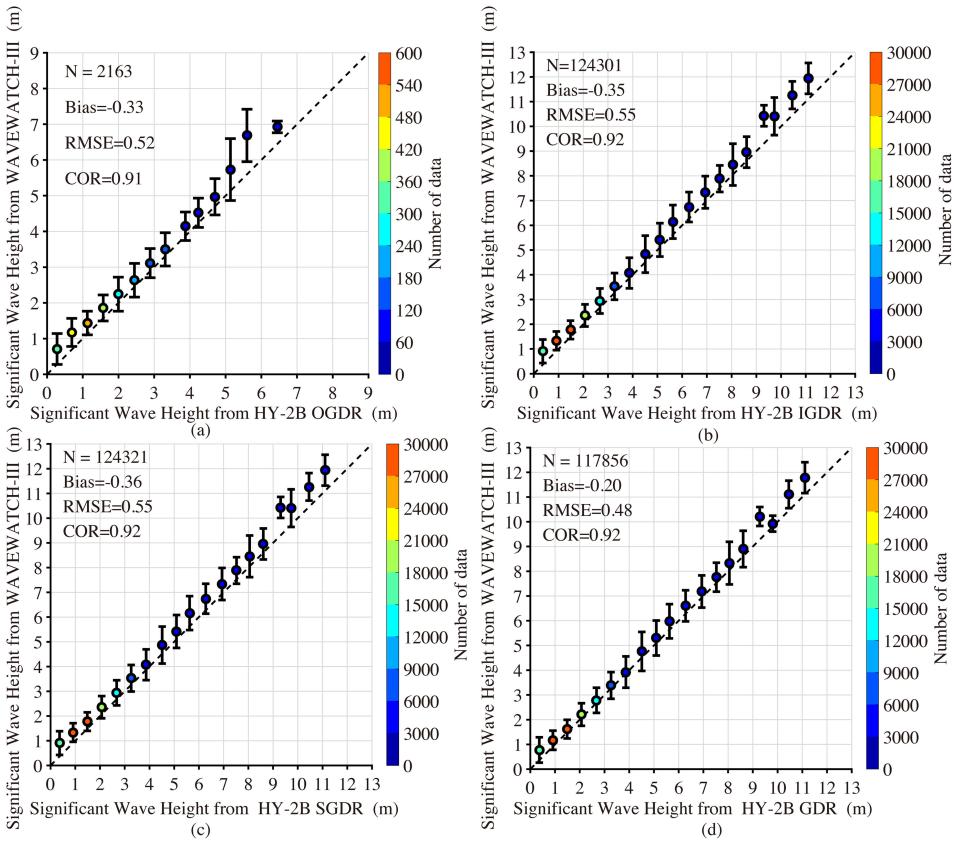

Fig. 14. Comparisons of SSH between HY-2B and the WW3 model for a 0.5 m bin. (a) Operational geophysical data record. (b) Interim geophysical data record. (c) Sensor geophysical data record. (d) Geophysical data record.

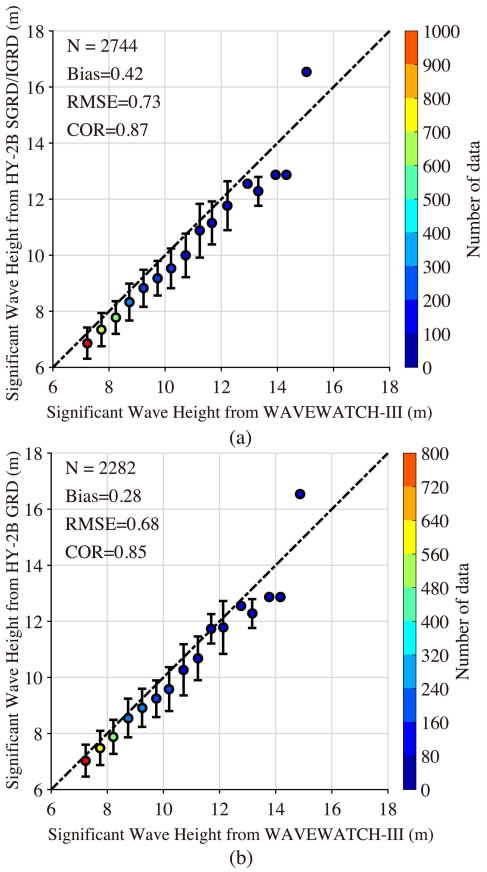

Fig. 15. Comparisons of SSH between Jason-3 and HY-2B for a 0.5 m bin in typhoons. (a) Operational geophysical data record. (b) Sensor geophysical data record. (c) Geophysical data record.

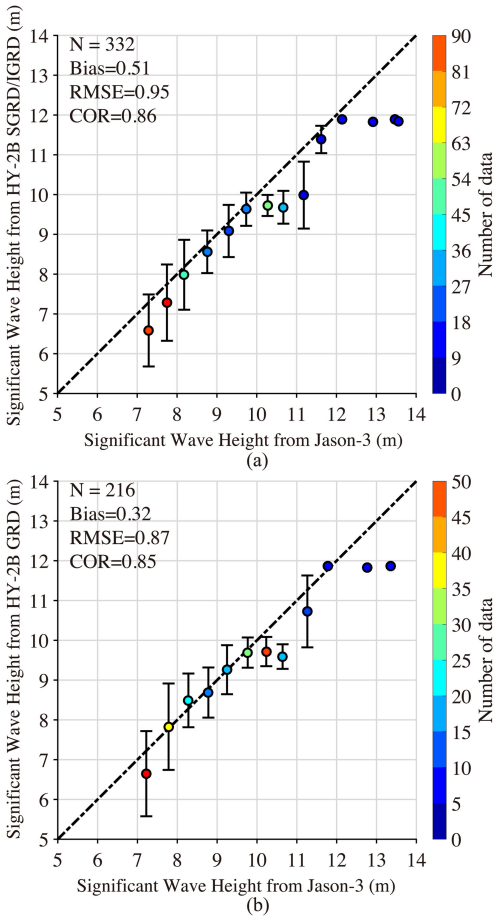

Fig. 16. Comparisons of SSH between WW3 and HY-2B for a 0.5 m bin in typhoons. (a) Operational geophysical data record and sensor geophysical data record. (b) Geophysical data record.

compared with the simulations from the WW3 model during typhoons at SWH >7 m. Analysis for more than two thousand matchups from two other types of data indicated that the GDR measurements performed better, with a 0.68 RMSE [see Fig. 16(b)], which was less than the 0.73 RMSE for both SGDR and IGDR [see Fig. 16(a)].

Collectively, we conclude that GDR is useful for wave monitoring at high sea states with SWH > 7 m, although the accuracy of extreme SWH (>12 m) awaits further confirmation due to insufficient samples available for this article.

IV. Discussions

In this section the differences in wind speed derived from the HY-2B scatterometer and SWH derived from GDR measurements derived from the HY-2B altimeter are compared in order to provide suggestions for improving the accuracy of HY-2B operational data. Fig. 17 shows the dependence of marine environmental parameters, i.e., HYCOM current speed for a 0.1 m/s bin [see Fig. 17(a)], HYCOM SST for a 2 °C bin [see Fig. 17(b)], GRAPS wind speed for a 1 m/s bin [see Fig. 17(c)], and WW3 SWH for a 0.3 m bin [see Fig. 17(d)] on the differences (ASCAT-measured wind speeds minus HY-measured wind speeds). The sea surface currents affected the difference in NRCS (±0.6 m/s) at current speeds greater than 1 m/s, indicating that currents modulate sea surface roughness under such conditions. Interestingly, the tendency of SST for the difference with NRCS was similar to that of wind speed for the difference in NRCS. We believe that the change of SST could affect the stability on the marine atmospheric boundary layer as well as hydrodynamic characteristics [42] and then the neutral wind speed. Moreover, the difference in NRCS increased significantly at wind speeds greater than 20 m/s. This kind of behavior also exists in the SAR wind retrieval [43] in the presence of ocean thermal fronts. At low sea states (SWH < 3 m), the difference in NRCS was less than 0.3 m, whereas the difference in NRCS increased at greater SWH conditions. Collectively, both HY-2B and ASCAT winds performed well at sea surface currents <1 m/s and SWH < 3 m; in particular, SST should be included in the wind retrieval for both HY-2B and ASCAT.

Similarly, Fig. 18 presents the relation between the difference of SWH (Jason-measured SWHs minus HY-measured SWHs) and these four parameters: HYCOM current speed; HYCOM SST; GRAPS; wind speed; and WW3 SWH. The difference of SWH remained at 0.1 m at HYCOM current speeds less than 2 m/s, while the difference of SWH became larger with increasing current speed. The HYCOM SST had less influence on the difference in SWH. The dependence on GRAPS winds indicates that the difference remained at 0.2 m with wind speeds

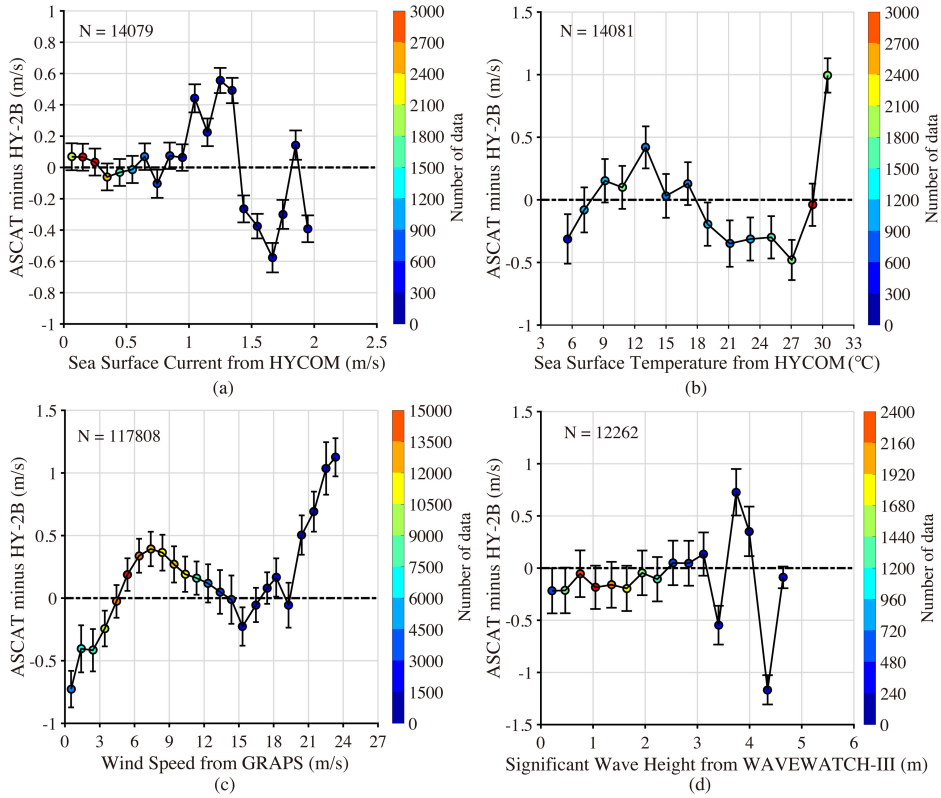

Fig. 17. Relation between the difference (ASCAT-measured wind speeds minus HY-measured wind speeds) and four parameters. (a) Sea surface current from the HYCOM model for a 0.1 m/s bin. (b) SST from HYCOM for a 2 °C bin. (c) GRAPS wind speed for a 1 m/s bin. (d) WW3 SWH for a 0.3 m bin.

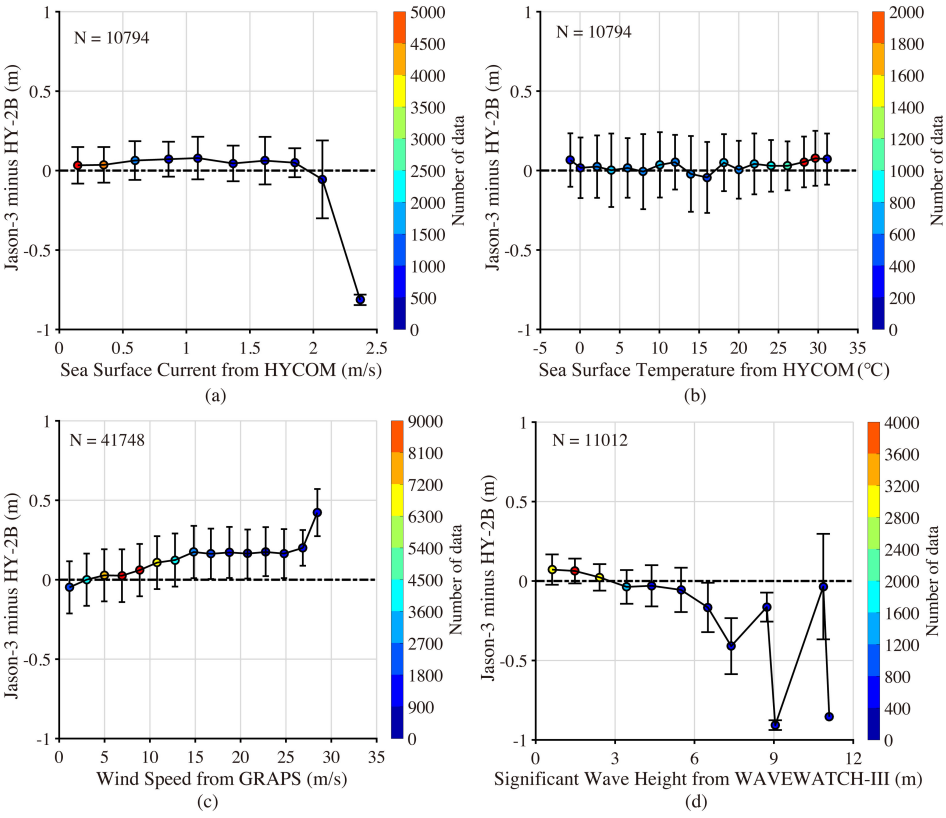

Fig. 18. Relation between the difference (Jason-measured SWHs minus HY-measured SWHs) and four parameters. (a) Sea surface current from HYCOM model for a 0.1 m/s bin. (b) SST from HYCOM for a 2 °C bin. (c) GRAPS wind speed for a 1 m/s bin. (d) WW3 SWH for a 0.3 m bin.

>10 m; in particular, the difference was less than 0.1 m at wind speeds <6 m. In addition, the difference in SWH was less than 0.1 m at SWH $<$ 3m; however, the difference increased with increasing SWH, especially at SWH $>$ 7 m. It is not surprising that wave state should determine the accuracy of altimeter waves as well as the results for HY-2B scatterometer winds.

V. Conclusion

The individual scatterometer and altimeter missions are designed for sea surface wind and wave monitoring over the global ocean. The Chinese HY-2B satellite launched in 2018 carries sensors for simultaneously obtaining wind speed and wave measurements. Moreover, wind data following the satellite footprints are also derived from the altimeter of HY-2B. Therefore, the objective of this article was to systemically evaluate operational winds and waves measured from HY-2B via calibration against other remote-sensing data, i.e., ASCAT winds and Jason-3 waves. In particular the performance of HY-2B under cyclonic conditions was investigated in order to confirm the applicability at high sea states in the China Seas. Note that four types of Level-2 data products derived from the HY-2B altimeter were employed, i.e., OGDR, IGDR, SGDR, and GDR. In order to calibrate the HY-measured SWH at high sea states, a well-known wave model, WW3, was used to simulate wave fields for 20 typhoons during the period from 2019 to 2020, where GRAPS winds were the forcing fields, and the comparisons between ECMWF and WW3-simulated SWHs showed a 0.47 m RMSE of SWH with a 0.81 COR.

The calibration of wind speeds (up to 25 m/s) from the HY-2B scatterometer against ASCAT showed a 0.78 m/s RMSE with a 0.97 COR, which was superior to the 1.2 m/s RMSE and 0.93 COR of winds from the GDR measurement by the HY-2B altimeter. The statistical errors of wind speed and SWH were analyzed using WW3-simulated SWH, HYCOM sea surface currents, and SST. The dependence of differences between ASCAT and HY-2B indicated that current and SST affected the scatterometer-measured winds at sea surface currents >1 m/s and SWH $>$ 3 m in particular, SST affected the scatterometer wind measurements by modulating the stability of the marine atmospheric boundary layer. It is more likely that the current and SST have less influence on altimeter waves, while the stage of the wave is the major controlling variable for HY-2B altimeter-measured waves.

We conclude that wind data from the HY-2B scatterometer are quite reliable at low-to-moderate wind speeds (<25 m/s). Moreover, SWH products from the GDR of the HY-2B altimeter performed best at low-to-high sea states, even during typhoons. In the near future we would promote a campaign of synchronous observations using HY-2B, the Chinese-French Oceanography Satellite, and GF-3 SAR satellites during the typhoon season in the western Pacific ocean, as this could provide an opportunity for sea surface dynamics research at high sea states.

Acknowledgment

The Haiyang-2B data were provided by the National Satellite Ocean Application Service through an authorized account via.[1] The winds from Global and Regional Assimilation and Prediction System were provided by the South China Sea Institute of Oceanology, the Chinese Academy of Sciences. The Advanced Scatterometer winds were downloaded via.[2] The wave data from altimeter Jason-3 mission were accessed via.[3] European Centre for Medium-Range Weather Forecasts wind and wave data were accessed via.[4] General Bathymetry Chart of the Oceans data were downloaded via: ftp.edcftp.cr.usgs.gov. The hybrid coordinate ocean model current, water level and sea surface temperature data were collected via.[5] We appreciate the National Centers for Environmental Prediction of the National Oceanic and Atmospheric Administration (NOAA) for providing the source code for the WAVEWATCH-III (WW3) model. The tracks of typhoons provided by Japan Meteorological Agency (JMA) were collected via.[6]

References

[1] J. J. W. Wilson *et al.*, "Radiometric calibration of the advanced wind scatterometer radar ASCAT carried onboard the METOP-A satellite," *IEEE Trans. Geosci. Remote Sens.*, vol. 48, no. 8, pp. 3236–3255, Jun. 2010.

[2] P. W. Gaiser *et al.*, "The windsat spaceborne polarimetric microwave radiometer: Sensor description and early orbit performance," *IEEE Trans. Geosci. Remote Sens.*, vol. 42, no. 11, pp. 2347–2361, Nov. 2004.

[3] F. G. Lemoine, N. P. Zelensky, D. S. Chinn, D. E. Pavlis, and V. Luceri, "Towards development of a consistent orbit series for Topex, Jason-1, and Jason-2," *Adv. Space Res.*, vol. 46, no. 12, pp. 1513–1540, Dec. 2010.

[4] S. Zhu *et al.*, "Evaluation of Chinese quad-polarization Gaofen-3 SAR wave mode data for significant wave height retrieval," *Can. J. Remote Sens.*, vol. 44, no. 6, pp. 588–600, Dec. 2018.

[5] N. Tran, P. Thibaut, J. C. Poisson, S. Philipps, E. Bronner, and N. Picot, "Impact of Jason-2 wind speed calibration on the sea state bias correction," *Mar. Geod.*, vol. 34, no. 3/4, pp. 407–419, Aug. 2011.

[6] W. Lin, M. Portabella, A. Stoffelen, A. Verhoef, and A. Turiel, "ASCATwind quality control near rain," *IEEE Trans. Geosci. Remote Sens.*, vol. 53, no. 8, pp. 4165–4177, Feb. 2015.

[7] X. M. Li, T. Koenig, J. Schulz-Stellenfleth, and S. Lehner, "Validation and intercomparison of ocean wave spectra inversion schemes using ASAR wave mode data," *Int. J. Remote Sens.*, vol. 31, no. 17/18, pp. 4969–4993, Sep. 2010.

[8] D. L. Pan, X. Q. He, S. Li, and G. Fang, "Study on application potentiality of the first China's ocean satellite HY-1A," *Acta Oceanol. Sin.*, vol. 22, no. 4, pp. 503–510, Dec. 2003.

[9] D. Pan, X. Q. He, and Q. K. Zhu, "In-orbit cross-calibration of HY-1A satellite sensor COCTS," *Chin. Sci. Bull.*, vol. 49, no. 12, pp. 2521–2526, Dec. 2004.

[10] L. Sun, J. Zhang, and M. Guo, "Influence analysis of gaseous absorption on 'HY—1A' CZI data processing simulation and correction for Rayleigh scattering," *Acta Oceanol. Sin.*, vol. 27, no. 6, pp. 102–114, Dec. 2008.

[11] H. Wang, J. H. Zhu, M. S. Lin, Y. G. Zhang, and Y. T. Chang, "Evaluating Chinese HY-2B HSCAT ocean wind products using buoys and other scatterometers," *IEEE Geosci. Remote Sens.*, vol. 17, no. 6, pp. 923–927, Jun. 2020.

[12] A. Stoffelen and D. Anderson, "Scatterometer data interpretation estimation and validation of the CMOD4," *J. Geophys. Res.*, vol. 102, no. 102, pp. 5767–5780, Jan. 1997.

[13] Y. Quilfen, A. Bentamy, T. Elfouhaily, K. Katsaros, and J. Tournadre, "Observation of tropical cyclones by high-resolution scatterometry," *J. Geophys. Res.*, vol. 103, no. C4, pp. 7767–7786, Jan. 1998.

[14] H. Hersbach, "Comparison of C-band scatterometer CMOD5.N equivalent neutral winds with ECMWF," *J. Atmos. Ocean Technol.*, vol. 27, no. 4, pp. 721–736, Apr. 2010.

[1] [Online]. Available: https://osdds.nsoas.org.cn
[2] [Online]. Available: http://archive.eumetsat.int
[3] [Online]. Available: https://data.nodc.noaa.gov
[4] [Online]. Available: http://www.ecmwf.int
[5] [Online]. Available: https://www.hycom.org
[6] [Online]. Available: http://www.jma.go.jp

[15] Y. Y. Yurovsky, V. N. Kudryavtsev, S. A. Grodsky, and B. Chapron, "Ka-band dual copolarized empirical model for the sea surface radar cross section," *IEEE Trans. Geosci. Remote Sens.*, vol. 55, no. 3, pp. 1629–1647, Dec. 2016.
[16] M. H. Pickett, W. Tang, L. K. Rosenfeld, and C. H. Wash, "Quikscat satellite comparisons with nearshore buoy wind data off the U.S. west coast," *J. Atmos. Ocean. Technol.*, vol. 20, no. 12, pp. 1869–1879, Dec. 2003.
[17] W. Lin, M. Portabella, A. Stoffelen, J. Vogelzang, and A. Verhoef, "ASCAT wind quality under high subcell wind variability conditions," *J. Geophys. Res.*, vol. 120, no. 8, pp. 5804–5819, Aug. 2015.
[18] J. T. Macklin and R. A. Cordey, "Seasat SAR observations of ocean waves," *Int. J. Remote Sens.*, vol. 12, no. 8, pp. 1723–1740, Aug. 1991.
[19] J. Wu, "Near-nadir microwave specular returns from the sea surface—Altimeter algorithms for wind and wind stress," *J. Atmos. Ocean. Technol.*, vol. 9, no. 5, pp. 659–667, Oct. 1992.
[20] X. Y. Xu, K. Xu, H. Shen, Y. L. Liu, and H. G. Liu, "Sea surface height and significant wave height calibration methodology by a GNSS buoy campaign for HY-2A altimeter," *IEEE J. Sel. Topics Appl. Earth Observ. Remote Sens.*, vol. 9, no. 11, pp. 5252–5261, Nov. 2016.
[21] X. M. Ye, M. S. Lin, and Y. Xu, "Validation of Chinese HY-2 satellite radar altimeter significant wave height," *Acta Oceanol. Sin.*, vol. 34, no. 5, pp. 60–67, May 2015.
[22] T. V. Martin, H. J. Zwally, A. C. Brenner, and R. A. Bindschadler, "Analysis and retracking of continental ice sheet radar altimeter waveforms," *J. Geophys. Res.*, vol. 88, no. C3, pp. 1608–1616, Feb. 1983.
[23] J. L. Bamber, "Ice sheet altimeter processing scheme," *Int. J. Remote Sens.*, vol. 15, no. 4, pp. 925–938, May 2007.
[24] M. Jiang, K. Xu, and Y. Liu, "Global statistical assessment and cross-calibration with Jason-2 for reprocessed HY-2A altimeter data," *Mar. Geod.*, vol. 41, no. 3, pp. 289–312, Mar. 2018.
[25] S. A. Bhowmick *et al.*, "Validation of SWH and SSHA from SAEAL/AltiKa using Jason-2 and in-situ observations," *Mar. Geod.*, vol. 38, pp. 193–205, Oct. 2015.
[26] G. Brown, "The average impulse response of a rough surface and its applications," *IEEE Trans. Antennas. Propag.*, vol. 25, no. 1, pp. 67–74, Jan. 1977.
[27] G. S. Hayne, "Radar altimeter mean return waveforms from near-normal-incidence ocean surface scattering," *IEEE Trans. Antennas. Propag.*, vol. AP-28, no. 5, pp. 687–692, Sep. 1980.
[28] J. Gourrion, D. Vandemark, S. Bailey, and B. Chapron, "A two-parameter wind speed algorithm for Ku-band altimeters," *J. Atmos. Ocean. Technol.*, vol. 19, no. 2, pp. 2030–2048, Feb. 2002.
[29] M. H. Sun, Y. H. Duan, J. R. Zhu, H. Wu, J. Zhang, and W. Huang, "Simulation of Typhoon Muifa using a mesoscale coupled atmosphere-ocean model," *Acta Oceanol. Sin.*, vol. 33, no. 11, pp. 123–133, Nov. 2014.
[30] Y. X. Sheng, W. Z. Shao, S. Q. Li, Y. M. Zhang, H. W. Yang, and J. C. Zuo, "Evaluation of typhoon waves simulated by WaveWatch-III model in shallow waters around Zhoushan islands," *J. Ocean Univ. China*, vol. 18, no. 2, pp. 365–375, Mar. 2019.
[31] Y. Y. Hu, W. Z. Shao, J. Shi, J. Sun, Q. Y. Ji, and L. N. Cai, "Analysis of the typhoon wave distribution simulated in WAVEWATCH-III model in the context of Kuroshio and wind-induced current," *J. Oceanol. Limnol.*, vol. 38, no. 6, pp. 1692–1710, Dec. 2020.
[32] Y. Y. Hu, W. Z. Shao, Y. L. Wei, and J. C. Zuo, "Analysis of typhoon-induced waves along typhoon tracks in the western North Pacific Ocean, 1998–2017," *J. Mar. Sci. Eng.*, vol. 8, no. 7, pp. 521, Jul. 2020.
[33] L. Y. Wan, J. Zhu, L. Bertino, and H. Wang, "Initial ensemble generation and validation for ocean data assimilation using HYCOM in the pacific," *Ocean Dyn.*, vol. 58, no. 3, pp. 81–99, May 2008.
[34] W. Z. Shao *et al.*, "Intelligent wind retrieval from Chinese Gaofen-3 SAR imagery in quad-polarization," *J. Atmos. Ocean. Technol.*, vol. 36, no. 11, pp. 2121–2137. Nov. 2019.
[35] S. Zhu, W. Z. Shao, A. Marino, J. Sun, and J. X. Z. Yuan, "Semi-empirical algorithm for wind speed retrieval from Gaofen-3 quad-polarization strip mode SAR data," *J. Ocean Univ. China*, vol. 19, no. 1, pp. 23–35, Jan. 2020.
[36] J. Vogelzang and A. Stoffelen, "ASCAT ultrahigh-resolution wind products on optimized grids," *IEEE J. Sel. Topics Appl. Earth Observ. Remote Sens.*, vol. 10, no. 5, pp. 2332–2339, May 2017.
[37] A. G. Voronovich and V. U. Zavorotny, "Full-polarization modeling of monostatic and bistatic radar scattering from a rough sea surface," *IEEE Trans. Antennas Propag.*, vol. 62, no. 3, pp. 1362–1371, Mar. 2014.
[38] P. A. Hwang, B. Zhang, J. V. Toporkov, and W. Perrie, "Comparison of composite Bragg theory and quad-polarization radar backscatter from RADARSAT2: With applications to wave breaking and high wind retrieval," *J. Geophys. Res.*, vol. 115, no. C11, pp. 246–255, Nov. 2010.
[39] Z. H. Yang, W. Z. Shao, Y. Ding, J. Shi, and Q. Y. Ji, "Wave simulation by the SWAN model and FVCOM considering the sea-water level around the Zhoushan islands," *J. Mar. Sci. Eng.*, vol. 8, no. 10, pp. 783, Oct. 2020.
[40] W. Z. Shao *et al.*, "Analysis of wave distribution simulated by WAVEWATCH-III model in typhoons passing Beibu Gulf, China," *Atmosphere*, vol. 9, no. 7, pp. 265, Jul. 2018.
[41] J. E. Stopa and K. F. Cheung, "Intercomparison of wind and wave data from the ECMWF reanalysis interim and the NCEP climate forecast system reanalysis," *Ocean Model*, vol. 75, no. 3, pp. 65–83, Mar. 2014.
[42] W. Z. Shao *et al.*, "Analysis of waves observed by synthetic aperture radar across ocean fronts," *Ocean Dyn.*, vol. 70, no. 9, pp. 1397–1347, Sep. 2020.
[43] Q. Xu, Y. Li, X. Li, Z. Zhang, Y. Cao, and Y. Cheng, "Impact of ships and ocean fronts on coastal sea surface wind measurements from the advanced scatterometer," *IEEE J. Sel. Topics Appl. Earth Observ. Remote Sens.*, vol. 11, no. 7, pp. 2162–2169, Jul. 2018.

Weizeng Shao (Member, IEEE) received the B.S. degree in engineering from the JiangSu University of Science and Technology, Zhenjiang, China, in 2007, and the Ph.D. degree in physical oceanography from the Ocean University of China, Qingdao, China, in 2013.

During his Ph.D. program, in 2010–2012, he was a Visiting Research Scientist with SAR oceanography Group, German Aerospace Center, Munich, Germany. From 2015 to 2020, he was an Associate Professor and the Master's student supervisor with Zhejiang Ocean University, Zhoushan, China. Since 2019, he has been an Assistant Researcher with National Satellite Ocean Application Service, Beijing, China. Since 2021, he has been a Full Professor with Shanghai Ocean University, Shanghai China. His research interests include marine applications using synthetic aperture radar, especially for Chinese Gaofen-3 (GF-3), HY-2, and CFOSAT, and ocean modeling for typhoons and hurricanes.

Tao Jiang received the B.S. degree from AnHui Science and Technology University, Huainan, China, in 2020. He is currently working toward the master's degree in physical oceanography with Shanghai Ocean University, Shanghai, China.

His research interests include ocean remote sensing and ocean modeling.

Xingwei Jiang received the Ph.D. degree in science in 2008.

He became an Academician of the Chinese Academy of Engineering and a Doctoral Supervisor. He is currently the Director of the Chinese National Satellite Marine Application Center and the Chief Designer of Chinese marine satellite ground application systems. He presided over the establishment of a marine satellite ground application system platform and formulated marine remote sensing technical regulations. He has authored or coauthored number of monographs, atlases, and papers, and formed a marine satellite ground application engineering technical team. He was the Vice Chairman of the Chinese Ocean Society and the China association for remote sensing applications. He was the Chairman of the Ocean Remote Sensing Professional committee of the Chinese ocean society and was a member of the International GEO Organization Technical Coordination Group and the Sino-French Marine Satellite Joint Steering Committee.

Youguang Zhang received the Ph.D. degree in ocean remote sensing fields from the Institute of Oceanology, Chinese Academy of Sciences, Beijing, China, in 2004.

He was the Deputy Chief of the Chinese HY-2 satellite ground system and the ocean salinity satellite ground system. He was a member of the marine satellite ground application system project. He has authored or co-authored more than 50 peer-reviewed papers on remote sensing. His research interests include satellite altimeter data processing and application research, satellite wave spectrometer data processing and application research, and the marine microwave remote sensor calibration technology research.

Wei Zhou received the Ph.D. degree in physical oceanography from the South China Sea Institute of Oceanology, Chinese Academy of Sciences, Beijing China, in 2011.

Since 2011, he has been an Assistant Research Fellow with Beijing Climate Center, Beijing, China. Since 2017, he has been an Associate Researcher with the South China Sea Institute of Oceanology. His research interests include ocean data assimilation and regional ocean modeling.